

# High Yield Synthesis of Molecular Brushes via ATRP in Miniemulsion

Ke Min,<sup>†</sup> Sherryll Yu,<sup>‡</sup> Hyung-il Lee,<sup>†</sup> Laura Mueller,<sup>†</sup> Sergei S. Sheiko,<sup>‡</sup> and Krzysztof Matyjaszewski<sup>\*,†</sup>

Center for Macromolecular Engineering, Department of Chemistry, Carnegie Mellon University, 4400 Fifth Avenue, Pittsburgh, Pennsylvania 15213, and Department of Chemistry, University of North Carolina at Chapel Hill, Chapel Hill, North Carolina 27599-3290

Received May 20, 2007; Revised Manuscript Received June 25, 2007

**ABSTRACT:** Molecular brushes were successfully synthesized in miniemulsion systems via activators generated by electron transfer (AGET) ATRP. Confinement of the polymerization reaction within miniemulsion droplets ( $D_{\text{hydro}} = 275 \pm 10$  nm) effectively avoided the problem of macroscopic gelation observed in bulk polymerization. The side-chain polymers grew rapidly from the backbones within the droplets which resulted in high monomer conversion in a relatively short time. Molecular visualization by AFM proved that a small amount of cross-linking did occur only at high monomer conversions. However, this microscopic gelation showed no effect on the miniemulsion stability, and therefore the synthesized materials can still be easily used. Thus, the miniemulsion approach leads to preparation of polymer brushes in higher yields as compared to bulk or solution processes.

## Introduction

Molecular brushes, also known as bottle brush polymers and densely grafted comblike copolymers, have recently received much attention, especially after controlled/living radical polymerization processes were broadly applied to the preparation of various well-defined polymers.<sup>1,2</sup> Through light scattering and molecular visualization by atomic force microscopy (AFM), it has been shown that macromolecular brushes are distinguishable from other polymers by their chain extended wormlike conformations which are stabilized by steric repulsion between the densely grafted side chains.<sup>3–5</sup> As the solution and bulk physical properties of these materials with complex intramolecular structure have begun to be examined,<sup>6–13</sup> a number of potential applications have emerged. These include impact-resistant materials, one-component replacements for hydrogels, elastomers, adhesives, stabilizers, dispersants, emulsifiers, compatibilizers, and materials for directed mineralization of inorganic nanocrystals and for the formation of high aspect ratio nanowires.<sup>14–20</sup> Furthermore, they help to better understand the structural control necessary to design synthetic polymer molecules for use in nanomechanical devices.<sup>21</sup>

Growing polymer chains from multifunctional macroinitiators is an interesting but challenging task. Synthesis of macromolecular brushes can be accomplished through three routes: homopolymerization of macromonomers (“grafting through”),<sup>22–28</sup> attachment of side chains to the backbone (“grafting onto”),<sup>7,29–31</sup> and grafting side chains from the backbone (“grafting from”).<sup>3,32–36</sup> In each of these three routes, controlled/living polymerization, including atom transfer radical polymerization (ATRP),<sup>37,38</sup> plays an important role in preparing well-defined polymer brushes. Compared to the “grafting through” method, “grafting from” polymerizations result in brush copolymers with high molecular weight side chains.<sup>24</sup> An additional benefit to this approach is that it does not require the synthesis of a macromonomer, which is the most difficult step in the “grafting

through” process.<sup>1</sup> “Grafting from” is also more favorable than the “grafting onto” method because the latter is limited in achievable grafting density due to steric hindrance; i.e., the remaining reactive sites are shielded by the polymers already attached to the backbone. “Grafting from” has already been successfully used to prepare densely grafted polymers and surface-modified nanoparticles.<sup>39,40</sup>

However, one limitation of “grafting from” by ATRP is the increased probability of cross-linking reactions between multifunctional macroinitiators, especially at high monomer conversions. In a bulk polymerization, the greater the functionality, the earlier the onset of gelation occurs. Although at the gel point the weight fraction of the connected polymer brushes is not high, the massive network already traps a large fraction of individual polymer brushes and monomers. This makes the obtained material very difficult to process.<sup>41,42</sup> Generally in order to avoid gel formation, one has to use a highly diluted system so that intermolecular cross-linking can be decreased. Using this rationale, controlled syntheses of molecular brush copolymers using “grafting from” a linear multifunctional macroinitiator via ATRP were successfully carried out in highly dilute systems using both solvent and monomer as diluents. While diluting the system offers one solution to prevent gel formation, the disadvantages of a highly diluted system are also obvious. In particular, the rate of polymerization decreases significantly, as shown by the long reaction time. Furthermore, low monomer conversion is necessary to avoid gel formation, resulting in a significant waste of monomers.

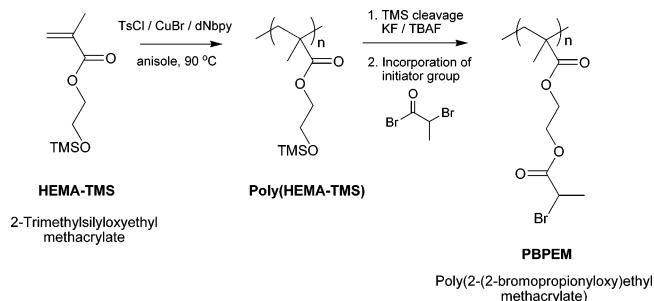
An alternative solution proposed in this paper is to use a miniemulsion system to synthesize macromolecular brushes. The final product from the miniemulsion polymerization is in the form of colloids protected by the surfactant layer.<sup>43–45</sup> Therefore, as long as the miniemulsion system remains stable, a macroscopic gel should not form. Cross-linking can still occur within the latex particles; however, it does not affect the fluidity of the miniemulsion system. Therefore, high monomer conversion can be achieved in miniemulsion ATRP without formation of the macroscopic gel.<sup>46</sup> The materials from miniemulsion can be redispersed and further processed.

\* Corresponding author. E-mail: km3b@andrew.cmu.edu.

<sup>†</sup> Carnegie Mellon University.

<sup>‡</sup> University of North Carolina at Chapel Hill.

## Scheme 1. pBPEM Macroinitiator Synthesis

Table 1. Synthesis of Polymer Brushes by ATRP of BA from pBPEM Macroinitiator<sup>a</sup>

entry	[BPEM]:[BA]:[CuBr <sub>2</sub> /BPMODA]:[reducing agent]	reducing agent	media
1	1:400:0.2 (Cu <sup>+</sup> ):0		bulk
2	1:400:0.4:0.2	Sn(EH) <sub>2</sub>	bulk
3	1:400:0.4:0.08	ascorbic acid	mini-emulsion
4	1:400:0.4:0.14	ascorbic acid	mini-emulsion
5	1:400:0.4:0.2	ascorbic acid	mini-emulsion
6	1:100:0.4:0.14	ascorbic acid	mini-emulsion

<sup>a</sup> Polymerization temperature: 80 °C. Miniemulsion conditions: [Brij 98]:[hexadecane] = 2.3/3.6% based on monomer; solid content = 20% (based on 100% conversion).

## Experimental Section

**Materials.** All chemicals were purchased from Aldrich and used as received unless otherwise stated. 2-(Trimethylsilyloxy)ethyl methacrylate (HEMA-TMS, 99%) was distilled under vacuum prior to use. CuBr (98%) was purified by stirring with glacial acetic acid followed by filtering and washing the resulting solid with isopropanol. 4,4'-Di(5-nonyl)-2,2'-bipyridine (dNbpy) was prepared as previously reported.<sup>47</sup> *n*-Butyl acrylate (BA, 99%) was purified by passing through a column filled with basic aluminum oxide to remove inhibitor, or antioxidant, in order to provide consistent kinetics in the presence of oxygen.<sup>48</sup> Bis(2-pyridylmethyl)octadecylamine (BPMODA) was synthesized according to the procedures previously published.<sup>49</sup>

**Preparation of Macroinitiators pBPEM.** Poly(2-(2-bromopropionyloxy)ethyl methacrylate) (pBPEM) was prepared as described previously and depicted in Scheme 1,<sup>3</sup> in which TsCl refers to tosyl chloride, KF to potassium fluoride, and TBAF to tetrabutylammonium fluoride.

**Synthesis of Molecular Brushes via Normal ATRP in Bulk.** Table 1 illustrates all experiments that are discussed in this paper. The Schlenk flask was charged with monomer BA (5.0 g), ligand BPMODA (0.0176 g), the macroinitiator pBPEM (0.026 g), and anisole (0.1 mL, as internal GC standard). The reaction mixture was deoxygenated by several freeze–pump–thaw cycles. After adding CuBr (0.0056 g) to the reaction mixture, the flask was immersed in an oil bath thermostated at 80 °C to initiate polymerization. The conversion was monitored by gas chromatography (GC) analysis.

**Synthesis of Molecular Brushes via AGET ATRP in Bulk.** The macroinitiator pBPEM (0.026 g), CuBr<sub>2</sub> (0.0087 g), and BPMODA (0.0176 g) were dissolved in BA (5.0 g) in a 10 mL Schlenk flask and purged with argon for 30 min. The flask was then immersed in an oil bath thermostated at 80 °C. A pre-deoxygenated anisole solution (0.4 mL) of tin(II) 2-ethylhexanoate (Sn(EH)<sub>2</sub>, 0.0079 g) was injected into the flask to initiate the reaction. The conversion was monitored by GC analysis.

**Synthesis of Molecular Brushes via AGET ATRP in Mini-emulsion.** In a typical run, the macroinitiator pBPEM (0.026 g), CuBr<sub>2</sub> (0.0087 g), and BPMODA (0.0176 g) were dissolved in BA

(5.0 g) in a round-bottom flask at 60 °C. After the formation of the Cu(II) complex, hexadecane (0.18 g) and an aqueous solution of Brij 98 (20 mL, 5 mmol/L) were added to the cooled solution before the mixture was subjected to sonication. The resulting homogenized suspension was transferred to a 25 mL Schlenk flask and purged with argon for 30 min. The flask was then immersed in an oil bath thermostated at 80 °C. An aqueous solution (0.5 mL) of ascorbic acid (0.0034 g) was injected into the flask (dropwise for ~15 min) to initiate the polymerization. Aliquots were taken at regular intervals to measure the conversion gravimetrically.

**Measurements.** <sup>1</sup>H NMR of the macroinitiator pBPEM, performed in CDCl<sub>3</sub> on a 300 MHz Bruker spectrometer with TMS as the standard, showed that essentially every repeating unit of the macroinitiator contained one bromoester group, i.e., quantitative initiation.

During polymerizations, conversion was determined gravimetrically in the case of miniemulsion polymerization and by gas chromatography (GC) in the case of bulk polymerization using a Shimadzu GC-14A gas chromatograph, equipped with a J&W Scientific 30 m DB-WAX column with a Shimadzu CR51 Chromatopac. After miniemulsion polymerization, the hydrodynamic size of latex particles (*D*<sub>hydro</sub>) was measured by dynamic light scattering (DLS) on a high performance particle sizer, model HP5001 from Malvern Instruments, Ltd.

The polymer samples were dissolved in THF and filtrated by 220 nm filters before they were subject to GPC analysis (Polymer Standards Services (PSS) columns (guard, 10<sup>5</sup>, 10<sup>3</sup>, and 10<sup>2</sup> Å), with THF eluent at 35 °C, flow rate = 1.00 mL/min, and differential refractive index (RI) detector (Waters, 2410)). The detectors employed to measure the absolute molecular weights (*M*<sub>w,MALLS</sub>) were a triple-detector system containing a RI detector (Wyatt Technology, Optilab REX), a viscometer detector (Wyatt Technology, ViscoStar), and a multiangle laser light scattering (MALLS) detector (Wyatt Technology, DAWN EOS) with the light wavelength at 690 nm. Absolute molecular weights were determined using ASTRA software from Wyatt Technology.

Dilute chloroform solutions of each brush sample were spun onto mica at 3000 rpm for ~2 min (Laurell Technologies Corp. model WS-400A-6NPP/Lite). The films were imaged in Tapping-mode using a Multimode atomic force microscope from Veeco Metrology group equipped with Nanoscope IIIA control station and silicon cantilevers from MikroMasch with resonance frequencies of about 160 kHz, spring constants of 5.0 N/m, and radii less than 10 nm. Molecular weights of some brush samples were determined using images of dense monolayer films prepared from the Langmuir–Blodgett technique<sup>50</sup> (KSV 5000 Instrument, Milli-Q double-distilled water  $\rho$  = 18.2 MΩ). A specially written computer software was used to analyze molecular dimensions from the captured micrographs.<sup>50</sup>

## Results and Discussion

The synthesis of macromolecular brushes using the “grafting from” method in the bulk systems must be stopped at low monomer conversions in order to avoid macroscopic gelation. To illuminate this, a normal ATRP of *n*-butyl acrylate (BA) was carried out in bulk using a poly(2-(2-bromopropionyloxy)ethyl methacrylate) (pBPEM, number of repeating monomer units *N* ~ 450) macroinitiator (Table 1, entry 1). The polymerization became visibly viscous after 20 min and then quickly transformed into a gel (the magnetic stirring bar could not move and nitrogen bubbles were trapped within the network) after 2 h. The monomer conversion was only ~23%. The polymerization continued after gelation, as can be seen from the kinetic plot (Figure 1). To avoid gelation, brush synthesis by normal ATRP is usually carried out in a very dilute system. Polymerization must be stopped at low monomer conversion because even in a highly diluted system there is still a possibility for cross-linking. Consequently, a significant amount of monomer

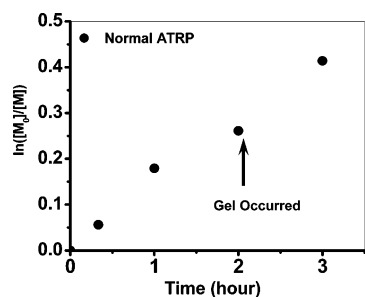


**Figure 1.** First-order kinetic plot for normal ATRP of BA with pBPfEM as macroinitiator in bulk. Polymerization condition: Table 1, entry 1.

and solvent is wasted, especially if a brush with long side chains is needed.

The problems of gelation are greatly alleviated when conducting ATRP in miniemulsion systems.<sup>51–53</sup> Compared with a bulk system, miniemulsion provides significant advantages for polymerizations conducted with multifunctional initiators. A high shearing force, such as sonication, is applied to an incompatible oil/water mixture to form uniform monomer droplets before polymerization is initiated. The oil in this system is a mixture of BA (monomer) and hexadecane (stabilizer). Therefore, a miniemulsion is a miniaturized bulk system with the reaction separated into small stable monomer droplets ranging in size from 50 to 500 nm.<sup>43</sup> However, in a miniemulsion system, intermolecular termination reactions cannot occur between molecules present in two different miniemulsion droplets, and therefore, macroscopic gelation does not occur. Even if some of the molecular brushes cross-link inside a droplet as the monomer conversion increases, cross-linking is confined only to that particular monomer droplet, and the obtained material can still be purified and processed afterward. In polymerizations from a multifunctional initiator, intramolecular termination takes place between two chains tethered to the same polymer backbone, which, in turn, competes with intermolecular termination and consequently postpones the occurrence of gelation in each colloid. Last but not least, applying ATRP in aqueous dispersed system such as miniemulsion is an environmentally friendly approach that is becoming industrially important in view of the tighter restrictions on solvent use.

In order to apply miniemulsion ATRP to the preparation of polymer brushes, the details of the initiation process should be carefully considered. For instance, several problems prevented a successful normal ATRP in miniemulsion using macroinitiators. The Cu(I) complex is air-sensitive, which makes it difficult to manipulate the reaction medium during the preinitiation steps, especially during sonication. In addition, the initiator should not be added together with Cu(I) species before sonication; otherwise, prereaction may occur. Moreover, the macroinitiator is usually insoluble in water and can only be dissolved in a nonpolar solvent such as anisole, resulting in inefficient dispersion when the initiator solution is injected into the miniemulsion after sonication. In the screening experiment, the macroinitiators floated to the surface of the miniemulsion and failed to initiate polymerization as designed. These macroinitiators slowly generated polymer brushes because of diffusion of monomer and catalysts; however, the polymerization outside the monomer droplets significantly reduced the stability of the miniemulsion.

To overcome the drawback of normal ATRP and prepare pure materials, ATRP with activators generated by electron transfer (AGET) was adopted for macromolecular brushes synthesis. Instead of a conventional radical initiator, a reducing agent was used to generate activators from the oxidatively stable Cu(II) complex by a redox reaction (Scheme 2).<sup>54–58</sup> Since all radicals

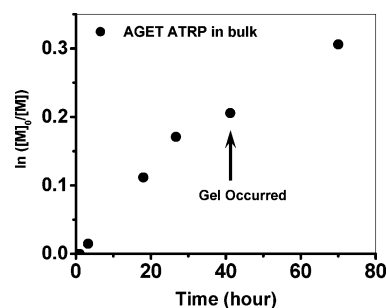
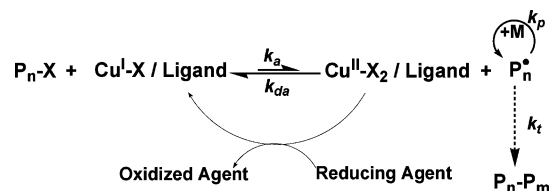


**Figure 2.** First-order kinetic plot for AGET ATRP of BA in bulk with pBPfEM as macroinitiator using Sn(EH)<sub>2</sub> as reducing agent. Polymerization condition: Table 1, entry 2.

#### Scheme 2. Proposed Mechanism of AGET ATRP



are generated by the reaction of the activators with the initiators along the backbone, no homopolymer chain formation was expected with this procedure. This AGET technique is especially beneficial for miniemulsion because the catalyst in the higher oxidation state is insensitive to air and survives sonication. The Cu(II) species and the macroinitiator can be encapsulated together inside monomer droplets during sonication, prior to the activation step.

For comparison purposes, an AGET ATRP was first carried out in bulk using tin(II) 2-ethylhexanoate (Sn(EH)<sub>2</sub>) as the reducing agent (Table 1, entry 2). The kinetic plot is shown in Figure 2.

Comparing Figure 1 and Figure 2, it can be concluded that the AGET ATRP was slower than that of normal ATRP because of the higher deactivator concentration maintained in the AGET system, which is usually beneficial for a good control over polymerization. According to Figure 2, the polymerization was faster at the beginning and slightly slower after ~20% conversion. Macroscopic gelation was observed after 42 h when the monomer conversion reached only ~20%. The polymerization was allowed to continue even after gelation occurred, and as the kinetic plot shows (Figure 2), the radical concentration, measured by the rate of polymerization, remained the same before and after gelation. However, the obtained product after 70 h was a cross-linked gel.

To prevent macroscopic gelation and the formation of an intractable material, AGET ATRP was applied in a miniemulsion for the synthesis of macromolecular brushes with ascorbic acid as the reducing agent (Table 1, entries 3–6). The reason for using a different reducing agent in miniemulsion is because of its hydrophilicity: ascorbic acid readily dissolves in water and rapidly reduces the Cu(II) complex. Because the resulting Cu(I) complexes are more hydrophobic than Cu(II) complexes, the reduction process essentially drives the active catalysts back into the droplets, providing more control during the polymerization. As previously reported, the ascorbic acid solution was slowly added to the system in order to eliminate the possibility of an early nonstationary period.<sup>55</sup>

As the kinetic plots show (Figure 3), the amount of reducing agent added to the reaction influenced the polymerization rate. When the ratio of ascorbic acid to Cu(II) complexes was increased from 0.2 to 0.35, more Cu(II) were reduced to Cu(I)



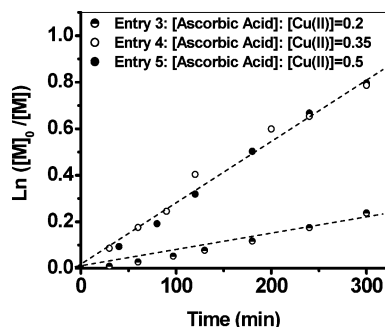


**Figure 3.** First-order kinetic plots for AGET ATRP of BA in miniemulsion with pBPfEM as macroinitiator using variable amounts of ascorbic acid as reducing agent. Polymerization condition: Table 1, entries 3–5.

complexes. This, in turn, increased the polymerization rate due to the resulting higher ratio of  $[Cu(I)]/[Cu(II)]$ . However, when

the amount of ascorbic acid was further increased, no obvious increase of polymerization rate was observed. All of the polymerizations resulted in stable miniemulsion without observed macroscopic gelation. The particle size of the miniemulsion was  $275 \pm 10$  nm. In each particle there were  $\sim 270$  brushes and  $\sim 110\,000$  growing chain ends (active and dormant).

According to kinetic plots in Figure 3, the overall radical concentration  $[R^*]$  was calculated (when the ratio of ascorbic acid to  $Cu(II)$  complexes was 0.35 or 0.5) to be  $9.2 \times 10^{-10}$  M (using  $k_p = 4.82 \times 10^4 \text{ M}^{-1} \text{ s}^{-1}$ ).<sup>59</sup> Based on the volume of miniemulsion droplet ( $1.04 \times 10^7 \text{ nm}^3$ ), the average number of propagating chains per droplet was  $5.8 \times 10^{-3}$ . This means, on average, 0.58% of droplets were “active” and 99.42% of the droplets were “inactive” with all alkyl halides at the dormant stage. For the ratio of ascorbic acid to  $Cu(II)$  complexes 0.2, only 0.17% of droplets were active. Therefore, the segregation of radicals could result in reduced probability of termination

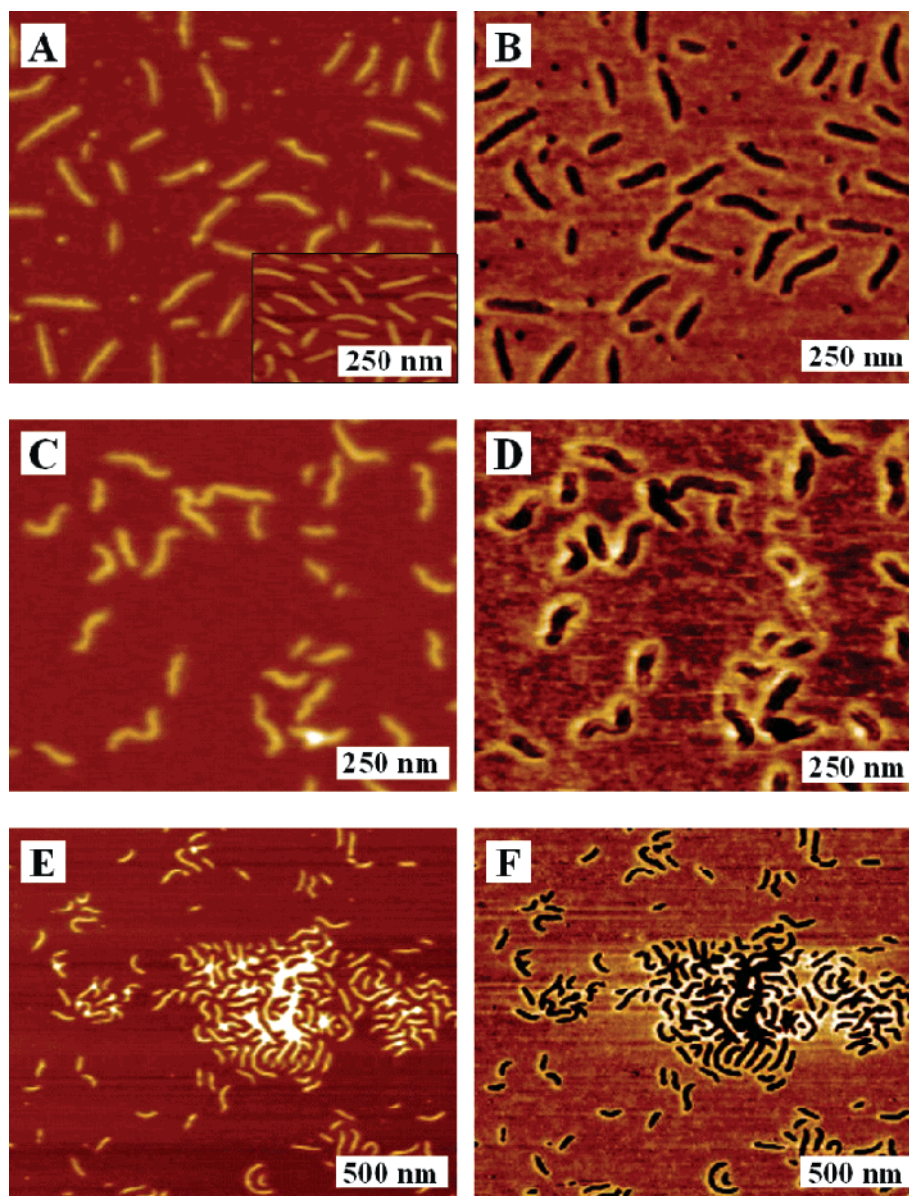


**Figure 4.** AFM images of brushlike polymers synthesized from AGET ATRP of BA from pBPfEM macroinitiator in miniemulsion with DP of the side chains  $n_{PBA} \sim 80$ . (A) Height and (B) phase images of brushes obtained from  $[ascorbic\ acid]:[Cu(II)] = 0.20$  after monomer conversion  $\sim 21\%$  (Table 1, entry 3). Inset is a dense monolayer film used for measuring the molecular weight and side chain length. (C) and (D) are the height and phase images, respectively, of brushes obtained from  $[ascorbic\ acid]:[Cu(II)] = 0.35$  after reaching  $\sim 25\%$  conversion (Table 1, entry 4). (E) Height and (F) phase images of brushlike polymers synthesized from AGET ATRP of BA from pBPfEM macroinitiator in miniemulsion taken at monomer conversion  $\sim 80\%$  (Table 1, entry 6). Individual and coupled brushes are present in this sample.

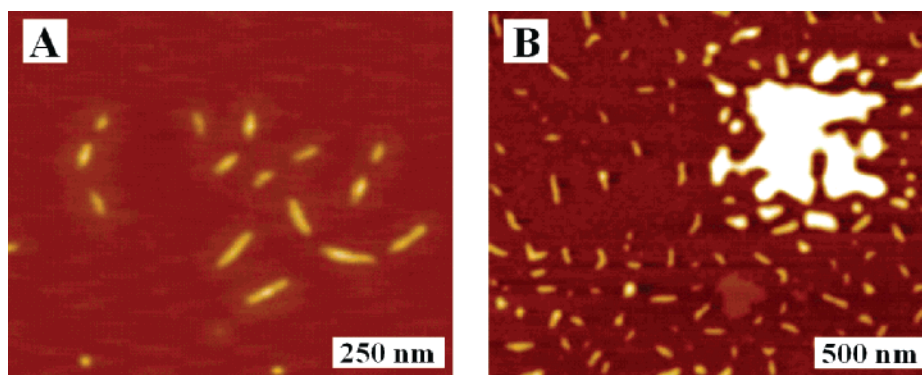


**Figure 5.** AFM images of brushlike polymers synthesized from AGET ATRP of BA from pBPBM macroinitiator in miniemulsion with [ascorbic acid]:[Cu(II)] = 0.35 (Table 1, entry 4). (A) Height images of brushlike polymers obtained at monomer conversion  $\sim 56\%$ . (B) Height images of brushlike polymers with monomer conversion  $\sim 84\%$ , which shows a both single molecules and nanogels present in the sample.

**Table 2. Summary of Results from Molecular Dimensional Analysis**

entry	% conv	$L_n$ , <sup>a</sup> nm	$l_m$ , <sup>b</sup> nm	PDI <sup>c</sup>	$d$ , <sup>d</sup> nm	$M_n$ <sup>e</sup> ( $\times 10^{-6}$ ), g/mol
3	21	$99 \pm 7$	$0.22 \pm 0.03$	$1.1 \pm 0.3$	$80 \pm 6$	$5 \pm 1$
4	25	$111 \pm 6$	$0.25 \pm 0.03$	$1.2 \pm 0.1$	$80 \pm 4$	$4 \pm 1$
6 <sup>f</sup>	80	$106 \pm 7$	$0.24 \pm 0.02$	$1.2 \pm 0.1$	$65 \pm 6$	
3	56	$94 \pm 8$	$0.21 \pm 0.03$	$1.2 \pm 0.4$	$115 \pm 7$	$6 \pm 1$
3 <sup>f</sup>	84	$75 \pm 6$	$0.17 \pm 0.03$	$1.3 \pm 0.2$	$150 \pm 10$	

<sup>a</sup> Number-average contour length. <sup>b</sup> Length per monomeric unit,  $L_n/N_{\text{backbone}}$ . <sup>c</sup> Polydispersity index,  $L_w/L_n$ . <sup>d</sup> Distance between brushes in a dense monolayer. <sup>e</sup> Number-average molecular weight by AFM/LB technique [*J. Am. Chem. Soc.* **2003**, *125*, 6725–6728]. <sup>f</sup> Unable to determine  $M_n$  because of the presence of nanogels.

(including intramolecular and intermolecular processes), according to the recent literature reports.<sup>60,61</sup>

AFM images prepared for the polymer brushes obtained when the ratio of ascorbic acid to Cu(II) complexes was set as 0.2 (Table 1, entry 3) and the conversion of BA was determined to be  $\sim 21\%$  after 6 h are shown in Figure 4A,B. All polymer brushes appear to be single macromolecules. The polymerization conducted in bulk under the same conditions did not reach this conversion before macroscopic gelation occurred, proving that intermolecular coupling reactions were indeed reduced in the miniemulsion droplets. From the AFM images, the number-average molecular weight of the brushes was calculated to be  $M_n = (5 \pm 1) \times 10^6$  g/mol, and the PDI =  $1.1 \pm 0.3$ .<sup>50</sup> The molecular weight of the brushes by GPC-MALLS was  $4.8 \times 10^6$  g/mol with PDI = 1.40, which is consistent with the empirical calculation above (see Supporting Information for GPC trace). In addition to molecular weight, we also analyzed linear dimensions of the brush molecules. With brush contour length  $L_N = 99 \pm 7$  nm and a backbone degree of polymerization  $N_{\text{backbone}} \cong 450 \pm 30$ , the average length per monomer unit was calculated to be  $l_m = L_N/N_{\text{backbone}} = 0.22 \pm 0.03$  nm, which confirms that the brushes are close to full extension ( $l_{\text{max}} \cong 0.25$  nm).<sup>4</sup> Using a dense monolayer of the sample (as shown in the inset of Figure 4A), the width of the corona is found to be  $d = 80 \pm 6$  nm, which corresponds to degree of polymerization  $n_{\text{PBA}} = 80/(2 \times 0.25) = 160$ . However, based on monomer conversion, the calculated  $n_{\text{PBA}}$  is  $400 \times 21\% = 84$ . The discrepancy is attributed to both incomplete initiation efficiency and the polydispersity of the side chains:<sup>4,62</sup> the width of brushes observed in AFM measurement is determined by the longest side chains, resulting in a larger corona width.

When the ratio of ascorbic acid to Cu(II) was increased to 0.35 (Table 1, entry 4), the polymerization reached  $\sim 25\%$  monomer conversion after only  $\sim 1.5$  h (as seen in the kinetic plots, Figure 3). Given the similar monomer conversion, the obtained brushes should have very similar size as discussed above (entry 3, conversion = 21%). However, with a higher concentration of reducing agent, and accordingly a higher

concentration of radicals, the radical termination reactions should be more pronounced. In other words, compared with entry 3, more brush coupling should be observed in entry 4, at a similar monomer conversion. In the AFM images shown in Figure 4C,D, both individual brushes and a small amount of what appears to be coupled brushes were present, indicating a slightly higher level of termination reactions. The brushes also take fully stretched conformation with  $L_N = 111 \pm 6$  nm and  $l_m = 0.25 \pm 0.03$  nm, values that are consistent with the results of the previous sample since the backbones are the same ( $N_{\text{backbone}} \cong 450 \pm 30$ ). The width of the corona was found to be  $d = 80 \pm 4$  nm with  $M_n = (4 \pm 1) \times 10^6$  g/mol, and the PDI =  $1.2 \pm 0.1$  (see Supporting Information for GPC trace).

In comparison, a brush size of  $n_{\text{PBA}} \sim 80$  can also be achieved using the conditions stated in Table 1, entry 6 (i.e., higher initial monomer concentration), and the polymerization was stopped at a conversion of 80%. Therefore,  $n_{\text{PBA}}$  should still be  $\sim 80$  like that in Figure 4A,C. However, the concentration of radicals in this system is significantly higher than in entry 4, and consequently, an even higher level of coupling between brushes is anticipated. This was proven by the AFM images shown in Figure 4E,F: the early stages of nanogels formation inside droplets can be clearly observed, indicating a significant level of termination reactions occurring in this system. Despite the apparent nanogel formation, single molecules are still present in the sample, and the following dimensions were determined to be  $L_N = 106 \pm 7$  nm and  $l_m = 0.24 \pm 0.02$  nm with a corona width  $d = 65 \pm 6$  nm. Furthermore, the fluidity of the entire miniemulsion system remained unaffected by these gels, and less than 1 wt % of macroscopic gelation was observed for this system.

When the ratio of ascorbic acid to Cu(II) was maintained at 0.35 (entry 4) and the polymerization was stopped at  $\sim 56\%$  monomer conversion, the majority of the polymers present are still single entities (Figure 5A). However, the image also indicates some of the side chains might have undergone coupling reactions, thus linking some brushes together (see GPC trace in Supporting Information). With  $d = 115 \pm 7$  nm from a dense



monolayer of the sample,  $n_{\text{PBA}} = 115/(2 \times 0.25) = 230$ , which is within error of that calculated from the monomer conversion ( $400 \times 56\% = 224$ ). Unlike brushes in Figure 4, the measured length of the backbone  $L_N = 94 \pm 8$  nm was notably shorter than the samples obtained at 25% conversion despite having the same backbone ( $N_{\text{backbone}} \cong 450 \pm 30$ ). This is attributed to scission of the covalent backbone of brushes with long side chains ( $n_{\text{PBA}} \geq 140$ ) due to physical attraction to high surface energy substrates.<sup>63</sup>

Again, using the same polymerization conditions as above (entry 4) but allowing the reaction to proceed to  $\sim 84\%$  monomer conversion, it is immediately apparent that there are nanogels in this sample (Figure 5B), a striking difference from the previous samples with lower monomer conversions at these synthetic conditions ( $>80\%$  conversion) but similar to that obtained from the experiment in entry 6, which had a higher radical concentration. This result was again expected, since at such a high conversion, there is a greater probability for side chains to start coupling and eventually cross-link to form the random pockets of nanogels, which occupy  $\sim 3\%$  of the volume observed by AFM. In addition to this observation, a number of the brushes appear to be fractured with  $L_N = 75 \pm 6$  nm.<sup>63</sup> The distance between the single brushes present in a dense monolayer was found to be  $d = 150 \pm 10$  nm, corresponding to  $n_{\text{PBA}} = 150/(2 \times 0.25) = 300$ . This is slightly shorter than the anticipation based on monomer conversion ( $400 \times 84\% = 336$ ), considering the difficulty of measurement of side chains after nanogel formation and the scarcity of the single molecules. Despite these complications, the miniemulsion system was able to retain its fluidity even at such a high monomer conversion. The individual droplets are still separated from each other, and less than 1 wt % macroscopic gels formed. The results of the analyses are summarized in Table 2.

## Conclusions

Molecular brushes were successfully synthesized in a miniemulsion system via AGET ATRP. The macroscopic gelation was observed for bulk ATRP but not detected in miniemulsion. The side-chain polymers grew from backbones rapidly in miniemulsion droplets. High monomer conversion was reached in relatively short time. Molecular visualization by AFM proved that some cross-linking did occur in miniemulsion droplets when the conversion was high ( $\sim 84\%$ ). However, this cross-linking showed no effect to the miniemulsion stability and fluidity, and therefore, the synthesized materials can be easily processed for further uses/applications.

**Acknowledgment.** This work was financially supported by the National Science Foundation (CBET 0609087 and CHE 05-49353) and the CRP Consortium at CMU. The authors thank Haifeng Gao for help on GPC MALLS analysis.

**Supporting Information Available:** GPC traces of the macroinitiator and polymer brushes. This material is available free of charge via the Internet at <http://pubs.acs.org>.

## References and Notes

- Zhang, M.; Mueller, A. H. E. *J. Polym. Sci., Part A: Polym. Chem.* **2005**, *43*, 3461–3481.
- Sumerlin, B. S.; Matyjaszewski, K. In *Macromolecular Engineering*; Matyjaszewski, K., Gnanou, Y., Leibler, L., Eds.; Wiley-VCH Verlag GmbH & Co. KGaA: Weinheim, Germany, 2007; Vol. 2, p 1103.
- Beers, K. L.; Gaynor, S. G.; Matyjaszewski, K.; Sheiko, S. S.; Moeller, M. *Macromolecules* **1998**, *31*, 9413–9415.
- Sheiko, S. S.; Moeller, M. *Chem. Rev.* **2001**, *101*, 4099–4123.
- Dziezok, P.; Sheiko, S. S.; Fischer, K.; Schmidt, M.; Moller, M. *Angew. Chem.* **1998**, *36*, 2812–2815.
- Gerle, M.; Fischer, K.; Roos, S.; Mueller, A. H. E.; Schmidt, M.; Sheiko, S. S.; Prokhorova, S.; Moeller, M. *Macromolecules* **1999**, *32*, 2629–2637.
- Subbotin, A.; Saariaho, M.; Ikkala, O.; Ten Brinke, G. *Macromolecules* **2000**, *33*, 3447–3452.
- Sheiko, S. S.; Prokhorova, S. A.; Beers, K. L.; Matyjaszewski, K.; Potemkin, I. I.; Khokhlov, A. R.; Moeller, M. *Macromolecules* **2001**, *34*, 8354–8360.
- Fischer, K.; Schmidt, M. *Macromol. Rapid Commun.* **2001**, *22*, 787–791.
- Neugebauer, D.; Zhang, Y.; Pakula, T.; Sheiko, S. S.; Matyjaszewski, K. *Macromolecules* **2003**, *36*, 6746–6755.
- Gallyamov, M. O.; Tartsch, B.; Khokhlov, A. R.; Sheiko, S. S.; Boerner, H. G.; Matyjaszewski, K.; Moeller, M. *Chem.—Eur. J.* **2004**, *10*, 4599–4605.
- Potemkin, I. I.; Khokhlov, A. R.; Prokhorova, S.; Sheiko, S. S.; Moeller, M.; Beers, K.; Matyjaszewski, K. *Macromolecules* **2004**, *37*, 3918–3923.
- Xu, H.; Shirvanyants, D.; Beers, K.; Matyjaszewski, K.; Dobrynin, A. V.; Rubinstein, M.; Sheiko, S. S. *Phys. Rev. Lett.* **2005**, *94*, 237801.
- Djalali, R.; Li, S.-Y.; Schmidt, M. *Macromolecules* **2002**, *35*, 4282–4288.
- Ying, Z.; Constantini, N.; Mierzwa, M.; Pakula, T.; Neugebauer, D.; Matyjaszewski, K. *Polymer* **2004**, *45*, 6333–6339.
- Lau, W.; Van Rheenen, P. R.; Bromm, K. A.; Fasano, D. M.; Tepe, T. R. *Polym. Prepr. (Am. Chem. Soc., Div. Polym. Chem.)* **2005**, *46*, 197–198.
- Retsos, H.; Gorodyska, G.; Kiri, A.; Stamm, M.; Creton, C. *Langmuir* **2005**, *21*, 7722–7725.
- Rathgeber, S.; Pakula, T.; Wilk, A.; Matyjaszewski, K.; Beers, K. L. *J. Chem. Phys.* **2005**, *122*, 124904/124901–124904/124913.
- Pakula, T.; Zhang, Y.; Matyjaszewski, K.; Lee, H.-i.; Boerner, H.; Qin, S.; Berry, G. C. *Polymer* **2006**, *47*, 7198–7206.
- Rathgeber, S.; Pakula, T.; Wilk, A.; Matyjaszewski, K.; Lee, H.-i.; Beers, K. L. *Polymer* **2006**, *47*, 7318–7327.
- Zubarev, A. Y.; Odenbach, S.; Fleischer, J. J. *Magn. Mater.* **2002**, *252*, 241–243.
- Tsukahara, Y.; Tsutsumi, K.; Yamashita, Y.; Shimada, S. *Macromolecules* **1990**, *23*, 5201–5208.
- Wintermantel, M.; Gerle, M.; Fischer, K.; Schmidt, M.; Wataoka, I.; Urakawa, H.; Kajiwar, K.; Tsukahara, Y. *Macromolecules* **1996**, *29*, 978–983.
- Yamada, K.; Miyazaki, M.; Ohno, K.; Fukuda, T.; Minoda, M. *Macromolecules* **1999**, *32*, 290–293.
- Neugebauer, D.; Zhang, Y.; Pakula, T.; Matyjaszewski, K. *Macromolecules* **2005**, *38*, 8687–8693.
- Neugebauer, D.; Theis, M.; Pakula, T.; Wegner, G.; Matyjaszewski, K. *Macromolecules* **2006**, *39*, 584–593.
- Neugebauer, D.; Zhang, Y.; Pakula, T. *J. Polym. Sci., Part A: Polym. Chem.* **2006**, *44*, 1347–1356.
- Ohno, S.; Matyjaszewski, K. *J. Polym. Sci., Part A: Polym. Chem.* **2006**, *44*, 5454–5467.
- Ryu, S. W.; Hirao, A. *Macromolecules* **2000**, *33*, 4765–4771.
- Muchtar, Z.; Schappacher, M.; Deffieux, A. *Macromolecules* **2001**, *34*, 7595–7600.
- Gao, H.; Matyjaszewski, K. *J. Am. Chem. Soc.* **2007**, *129*, 6633–6639.
- Cheng, G.; Boker, A.; Zhang, M.; Krausch, G.; Muller, A. H. E. *Macromolecules* **2001**, *34*, 6883–6888.
- Boerner, H. G.; Beers, K.; Matyjaszewski, K.; Sheiko, S. S.; Moeller, M. *Macromolecules* **2001**, *34*, 4375–4383.
- Boerner, H. G.; Duran, D.; Matyjaszewski, K.; da Silva, M.; Sheiko, S. S. *Macromolecules* **2002**, *35*, 3387–3394.
- Qin, S.; Matyjaszewski, K.; Xu, H.; Sheiko, S. S. *Macromolecules* **2003**, *36*, 605–612.
- Fu, G. D.; Kang, E. T.; Neoh, K. G.; Lin, C. C.; Liaw, D. J. *Macromolecules* **2005**, *38*, 7593–7600.
- Wang, J.-S.; Matyjaszewski, K. *J. Am. Chem. Soc.* **1995**, *117*, 5614–5615.
- Matyjaszewski, K.; Xia, J. *Chem. Rev.* **2001**, *101*, 2921–2990.
- Pyun, J.; Kowalewski, T.; Matyjaszewski, K. *Macromol. Rapid Commun.* **2003**, *24*, 1043–1059.
- Matyjaszewski, K.; Dong, H.; Jakubowski, W.; Pietrasik, J.; Kusumo, A. *Langmuir* **2007**, *23*, 4528–4531.
- Pyun, J.; Jia, S.; Kowalewski, T.; Patterson, G. D.; Matyjaszewski, K. *Macromolecules* **2003**, *36*, 5094–5104.
- Matyjaszewski, K. *Polym. Int.* **2003**, *52*, 1559–1565.
- Sudel, E. D.; El-Aasser, M. S. In *Emulsion Polymerization and Emulsion Polymers*; Lovell, P. A., El-Aasser, M. S., Eds.; John Wiley & Sons: New York, 1997; p 707.
- Antonietti, M.; Landfester, K. *Prog. Polym. Sci.* **2002**, *27*, 689–757.

- (45) Asua, J. M. *Prog. Polym. Sci.* **2002**, 27, 1283–1346.
- (46) Bombalski, L.; Min, K.; Tang, C.; Matyjaszewski, K. *Polym. Prepr.* **2005**, 46, 359–360.
- (47) Matyjaszewski, K.; Patten, T. E.; Xia, J. *J. Am. Chem. Soc.* **1997**, 119, 674–680.
- (48) Gnanou, Y.; Hizal, G. *J. Polym. Sci., Part A: Polym. Chem.* **2003**, 42, 351–359.
- (49) Xia, J.; Matyjaszewski, K. *Macromolecules* **1997**, 30, 7697–7700.
- (50) Sheiko, S. S.; da Silva, M.; Shirvanyants, D.; LaRue, I.; Prokhorova, S.; Moeller, M.; Beers, K.; Matyjaszewski, K. *J. Am. Chem. Soc.* **2003**, 125, 6725–6728.
- (51) Qiu, J.; Charleux, B.; Matyjaszewski, K. *Prog. Polym. Sci.* **2001**, 26, 2083–2134.
- (52) Cunningham, M. F. *C. R. Chim.* **2003**, 6, 1351–1374.
- (53) Li, M.; Matyjaszewski, K. *J. Polym. Sci., Part A: Polym. Chem.* **2003**, 41, 3606–3614.
- (54) Jakubowski, W.; Matyjaszewski, K. *Macromolecules* **2005**, 38, 4139–4146.
- (55) Min, K.; Gao, H.; Matyjaszewski, K. *J. Am. Chem. Soc.* **2005**, 127, 3825–3830.
- (56) Min, K.; Jakubowski, W.; Matyjaszewski, K. *Macromol. Rapid Commun.* **2006**, 27, 594–598.
- (57) Oh, J. K.; Tang, C.; Gao, H.; Tsarevsky, N. V.; Matyjaszewski, K. *J. Am. Chem. Soc.* **2006**, 128, 5578–5584.
- (58) Hizal, G.; Tunca, U.; Aras, S.; Mert, H. *J. Polym. Sci., Part A: Polym. Chem.* **2006**, 44, 77–87.
- (59) Beuermann, S.; Buback, M. *Prog. Polym. Sci.* **2002**, 27, 191–254.
- (60) Charleux, B. *Macromolecules* **2000**, 33, 5358–5365.
- (61) Kagawa, Y.; Zetterlund, P. B.; Minami, H.; Okubo, M. *Macromol. Theory Simul.* **2006**, 15, 608–613.
- (62) Neugebauer, D.; Sumerlin, B. S.; Matyjaszewski, K.; Goodhart, B.; Sheiko, S. S. *Polymer* **2004**, 45, 8173–8179.
- (63) Sheiko, S. S.; Sun, F. C.; Randall, A.; Shirvanyants, D.; Rubinstein, M.; Lee, H.-i.; Matyjaszewski, K. *Nature (London)* **2006**, 440, 191–194.

MA071137D